Multiple ancestral and a plethora of recent gene duplications during the evolution of the green sensitive opsin genes (*RH2*) in teleost fishes

Zuzana Musilova[1] and Fabio Cortesi[2]

[1] Department of Zoology, Faculty of Science, Charles University, Vinicna 7, 12844 Prague, Czech Republic

[2] Queensland Brain Institute, The University of Queensland, Brisbane, QLD 4072, Australia

Corresponding author emails: zuzmus@gmail.com, fabio.cortesi@uqconnect.edu.au

Abstract

Vertebrates have four visual cone opsin classes that, together with a light-sensitive chromophore, provide sensitivity from the ultraviolet to the red wavelengths of light. The rhodopsin-like 2 (RH2) opsin is sensitive to the centre blue-green part of the spectrum, which is the most prevalent light underwater. While various vertebrate groups such as mammals and sharks have lost the *RH2* gene, in teleost fishes this opsin has continued to proliferate. By investigating the genomes of 115 teleost species, we find that *RH2* shows an extremely dynamic evolutionary history with repeated gene duplications, gene losses and gene conversion affecting entire orders, families and species. At least four ancestral duplications provided the substrate for today's *RH2* diversity with duplications occurring in the common ancestors of Clupeocephala, Neoteleostei, and Acanthopterygii. Following these events, *RH2* has continued to duplicate both in tandem and during lineage specific genome duplications. However, it has also been lost many times over so that in the genomes of extant teleosts, we find between zero to eight *RH2* copies. Using retinal transcriptomes in a phylogenetic representative dataset of 30 species, we show that *RH2* is expressed as the dominant green-sensitive opsin in almost all fish lineages. The exceptions are the Osteoglossomorpha (bony tongues and mooneyes) and several characin species that have lost *RH2*, and tarpons, other characins and gobies which do not or only lowly express the gene. These fishes instead express a green-shifted long-wavelength-sensitive *LWS* opsin. Our study highlights the strength of using modern genomic tools within a comparative framework to elucidate the detailed evolutionary history of gene families.

Introduction

Vertebrates use vision to find food and mates, avoid predators and to navigate their surroundings. At the centre of their visual systems lie the visual pigments which consist of an opsin receptor protein that is covalently bound to a vitamin A derived, light sensitive chromophore (Hunt et al., 2014; Wald, 1968). Five opsin types were already present in the vertebrate ancestor which can be distinguished by their photoreceptor specificity, their phylogeny and their maximum light sensitivity (λ_{max}) (Lamb, 2013). The rod or rhodopsin (RH1) is sensitive to the blue-green light spectrum ~ 450 – 540 nm λ_{max} and is expressed in the highly sensitive rod photoreceptors, which are active during dim light. Four cone-specific opsins are active during bright light conditions and confer spectral sensitivity from the ultraviolet (UV) to the red spectrum. These are the short-wavelength-sensitive 1 (SWS1, 345 – 440 nm λ_{max}), SWS2 (395 – 490 nm λ_{max}), rhodopsin-like 2 (RH2, 450 – 540 nm λ_{max}), and the long-wavelength-sensitive (LWS, 490 – 575 nm λ_{max}) (reviewed in Carleton et al., 2020; Yokoyama, 2008). As opposed to terrestrial vertebrates where the ancestral five opsins have either been maintained (e.g., birds) or some types might have been lost (e.g., mammals) (Hunt et al., 2014), in teleost fishes opsin genes have continued to proliferate at an astonishing rate (reviewed in Musilova et al., 2021). Amongst the cone opsins, *RH2* appears to have the highest number of gene duplicates in teleosts, with eight copies found in squirrel and soldierfishes (Holocentridae) (Musilova et al., 2019).

RH2-based visual pigments are sensitive to the middle of the light spectrum (blue to green) (Yokoyama and Jia, 2020), which is the most commonly available light underwater, especially with increasing depth (Jerlov, 1976; Munz and McFarland, 1977). As light is quickly scattered and absorbed in aquatic environments, deeper bodies of water lack shorter and longer wavelengths of light with fishes in those habitats often lacking the UV sensitive *SWS1* and red sensitive *LWS* genes but instead they have an increased number of *RH2* duplicates (Musilova et al., 2019). Similarly, species that are active during the night or during twilight hours, where blue to green light dominates, show increased reliance on *RH2* genes. As for the deeper living species, crepuscular and nocturnal fishes have often lost or do not express the genes sensitive to the edges of the visible light spectrum such as found in coral reef squirrel and soldierfishes (Busserolles et al., 2021) and cardinalfishes (Apagonidae) (Luehrmann et al., 2019). *RH2* and *RH1* share a common ancestry (reviewed in Musilova et al., 2021), and in the deep-sea pearlsides (*Maurolicus* spp.) *RH2* is expressed in rod-like cone cells (de Busserolles et al., 2017). Pearlsides are active during dusk and dawn when they come to the surface to feed while for the remainder of the time, they sink to a depth of around 200 m to rest (Giske et al., 1990).

It is during these twilight hours, when the light environment is blue shifted and at an intensity that is neither ideal for cone nor rod cells, that the transmuted rod-like cones seem to function at their best (de Busserolles et al., 2017). In the extreme case of deep-sea fishes, *RH2* is often the only remaining cone opsin gene in their genomes, where it is mostly expressed in the larval stages that start their lives in the shallow and well-lit epipelagic ocean (Lupše et al., 2021).

Interestingly, in the Osteoglossomorpha (bony tongues and mooneyes) and several characin species, *RH2* has been lost over evolutionary time and green sensitivity has been acquired by a modified, shorter-wavelength sensitive copy of the *LWS* opsin gene (Escobar-Camacho et al., 2020; Liu et al., 2018). This is similar to what occurred in primates including humans, whereby *RH2* was lost in the mammalian ancestor and green vision was recovered by means of a second, mid-wavelength sensitive (MWS) *LWS* duplicate (Carvalho et al., 2017; Yokoyama and Yokoyama, 1990). In gobies and most characins, *RH2* is still present, but nonetheless green sensitivity has been taken over by shorter shifted *LWS* duplicates (Cortesi et al., 2021; Escobar-Camacho et al., 2020). This shows that the spectral sensitivity range and function for specific types of opsins might not be as conserved as was previously assumed, calling for a more thorough investigation of this diverse gene family.

To understand the function of *RH2* more thoroughly and gain a comprehensive overview of the dynamics underlying the *RH2* evolution in fishes, we set out and mined publicly available genomes from a phylogenetic representative dataset of 115 teleost species. In doing so we uncover a rich evolutionary history that is characterised by multiple ancestral duplications and a plethora of more recent duplications, gene losses and gene conversion. Combined with retinal transcriptomes from 30 species, we show that *RH2* is expressed in the majority of fish species, but we also uncover a number of cases where its function has been taken over by other opsin genes, namely *LWS*.

Results and Discussion

Mining the genomes of 115 teleost species (and three non-teleost outgroups) and reconstructing the most extensive *RH2* phylogeny to date, we find that ray-finned fishes possess a median number of three *RH2* copies per species, thus making it the most numerous opsin gene in teleost fishes (Figs. 1 and 2, and Fig. S1). We also confirm that the blackbar soldierfish, *Myripristis jacobus*, with eight *RH2*s, has the highest number of paralogs in its genome (also see Musilova et al., 2019). Moreover, several species were found to have up to seven *RH2* duplicates including the milkfish (*Chanos chanos*) and the glacier lanternfish (*Benthosema glaciale*). However, other than the previously reported Osteoglossomorpha (Liu et al., 2018) and several

102 characin species (Escobar-Camacho et al., 2020), we did not find any species that has lost *RH2*
103 altogether (Fig. 1). Instead, based on retinal transcriptomes in 30 species, we discovered several
104 species and entire lineages where *RH2* is not or only minimally expressed, at least in the adult
105 stages (Fig. 3).

106 The phylogenetic reconstruction showed that the teleost ancestor most likely possessed
107 only one copy of *RH2*. Alternatively, *RH2* duplicates that could have existed in these early
108 fishes, might have been lost over evolutionary time and we are no longer able to detect them
109 in extant species. The first ancestral duplication that we find in our dataset dates to the ancestor
110 of Clupeocephala i.e., after the split of the Elopomorpha and Osteoglossomorpha lineages. At
111 this point, at least two but possibly even three rounds of gene duplications gave rise to four
112 ancestral *RH2* copies (Fig. 1). Two of these, *RH2-II* and *RH2-III*, are only found in the
113 Otomorpha lineage (herring, zebrafish, carp, knifefish, catfish and relatives) and were lost in
114 euteleosts (Figs. 1 and 2). A third copy (*RH2-I*) is found in a limited number of species
115 belonging to phylogenetically very distinct lineages including zebrafish (Cypriniformes,
116 Otomorpha), milkfish (Gonorynchiformes, Otomorpha), smelts (Osmeriformes, Euteleostei),
117 and squirrel and soldierfishes (Holocentriformes, Euteleostei). The fourth ancestral copy, by
118 convention referred to as *RH2*, served as the starting point for the immense diversification of
119 the green-sensitive opsins in euteleosts (Figs.1 and 2). Hence, the onset of the *RH2*
120 duplications, or more likely the surviving ancestral duplicates are from a different evolutionary
121 time point compared to the other visual opsins (Musilova et al., 2021). Both, the ancestral
122 duplicates of *RH1* (Chen et al., 2018; Musilova et al., 2019) and *LWS* (Cortesi et al., 2021) can
123 be dated back to the teleost ancestor or even earlier. On the contrary, the surviving ancestral
124 *SWS2* duplicates first occurred later during the teleost evolution, in the neoteleost and
125 percomorph ancestors (Cortesi et al., 2015).

126 Following the ancestral duplication events, the evolution of *RH2* appears even more
127 dynamic with numerous gene duplications and gene losses that occurred also in more recent
128 evolutionary times (Fig. 1 and Fig. S1). For example, differences between species of the same
129 order such as in the Carangiformes, Gobiiformes, and Clupeiformes are quite common (Fig.
130 S1). Interestingly, while in the Otomorpha this diversity is based on all four ancestral duplicates
131 (Fig. 2A), in euteleosts most of the *RH2* diversity stems from subsequent duplications of the
132 fourth ancestral *RH2* copy (Fig. 1). First, a gene duplication in the Neoteleostei ancestor gave
133 rise to the *RH2A* gene. The second copy from this event then duplicated again in the ancestor
134 of acanthopterygians, giving rise to the *RH2B* and *RH2C* copies (Fig. 1). The occurrence of the
135 *RH2A* and *RH2B* copies is common in percomorph fishes and has been widely reported in

136 previous opsin gene studies (reviewed in Lin et al., 2017; Musilova et al., 2021; Rennison et
137 al., 2012). In this study we identify for the first time a third percomorph-specific copy, *RH2C*,
138 which is present in numerous species including tunas, trevallies, labrids and sunfish (Fig. 1 and
139 Fig. S1). *RH2C* was likely lost in the ancestor of Ovalentaria, and this might explain why it has
140 been overlooked in previous studies as it is not found in many of the commonly studied model
141 species for vision such as medaka (Matsumoto et al., 2020), cichlids (Carleton and Yourick,
142 2020), killifish (Chang et al., 2021) and dottybacks (Cortesi et al., 2016). Finally, pikes
143 (Esociformes) and salmonids (Salmoniformes), the first lineages to split from the euteleosts,
144 have undergone independent duplications of the fourth ancestral *RH2* copy (Figs. 1 and 2B)
145 and do not share *RH2* paralogs with the otomorphs (*RH2-I, II* and *III*) or the neoteleosts (*RH2A,*
146 *B* and *C*).

147 Most of the *RH2* genes are found within the same genomic clusters (data not shown).
148 There are two main *RH2* synteny groups in teleosts. In the majority of euteleost species all *RH2*
149 genes occur in tandem on the same chromosomal cluster flanked by the *synpr* and *slc6A13*
150 genes. The Otomorpha *RH2-I* and *RH2-III* copies are also located in the same cluster with the
151 same flanking genes, while the *RH2-II* copy is located in a different cluster next to *mutS-H5*.
152 In some species which experienced whole genome duplications there are two highly similar
153 *RH2* clusters (e.g., in goldfish, *Carassius auratus*). However, only a single *RH2* cluster is
154 present in Salmoniformes, despite salmon also having undergone a lineage specific whole
155 genome duplication (Ss4R) (Lien et al., 2016). In very few cases such as in darters (*Etheostoma*
156 spp.) and pike (*Esox lucius*), we found that their *RH2* clusters were surrounded by different
157 genes. In these instances, it is likely that genomic rearrangements have affected the *RH2*
158 clusters. Alternatively, *RH2* copies might have moved around the genome with the help of
159 transposable elements before subsequent duplications took place.

160 *RH2* genes also appear strongly impacted by gene conversion (reviewed in Musilova et
161 al., 2021). Gene conversion, that is the unidirectional exchange of genetic information between
162 similar gene copies, may homogenise opsin gene coding regions by replacing parts of the
163 original gene with its paralog (e.g., Cortesi et al., 2015; Sandkam et al., 2017). Two ancestrally
164 differentiated copies might then appear like recently duplicated genes in the gene trees, as
165 observed in our dataset. For example, the three *RH2s* (two *RH2A* and one *RH2B*) found in
166 many percomorphs might have a common origin, but the synteny is not consistent between
167 species; in some cases one of the genes is arranged in the reverse directions other times, it is
168 not (Musilova et al., 2019) (Fig. 1). To resolve the true relationship between *RH2* paralogs that
169 have experienced gene conversion, several studies took the approach of removing the

converted parts of the genes before tree reconstruction. This has shown that for example the *RH2A* paralogs found in Amazonian cichlids have a shared ancestry with the *RH2A* paralogs in African and Neotropical cichlids (Escobar-Camacho et al., 2017). Also, in the spotted unicornfish, *Naso brevirostris*, removing the converted regions recovered the sister relationship between its *RH2A* and *RH2B* copies (Tettamanti et al., 2019). In general, gene conversion appears to be an important evolutionary mechanism for visual opsins [e.g., for *SWS2* (Cortesi et al., 2015), and *LWS* (Cortesi et al., 2021; Escobar-Camacho et al., 2020; Sandkam et al., 2017)], that quite possibly assists in keeping their function restricted to a certain spectral-sensitivity range.

Indeed, using gene expression from retinal transcriptomes in 30 species representing the breath of the teleost phylogeny, we show that *RH2* is the dominantly expressed green sensitive opsin gene in most teleost species (Fig. 3). This highlights the importance of *RH2* opsins for vision in different habitats ranging from clear streams over murky lakes to the relative darkness of the deep sea. However, in species which have lost (Osteoglossomorpha and some of the characins) or do not express (most characins and gobies) *RH2*, shorter wavelength shifted copies of the *LWS* opsin have taken up the green sensitive niche (also see Liu et al. 2018, Escobar-Camacho et al. 2020, and Cortesi et al. 2021).

It is important to note that it is the recent advances in whole genome sequencing and particularly the high-quality genomes produced by long-read sequencing and advanced assembly pipelines (e.g., Rhie et al., 2021), which have made it possible to gain a thorough overview of the evolutionary history of the teleost *RH2* opsin genes. Conventional short-read based assemblies often failed in the regions with multiple *RH2*s due to the high similarity between copies, numerous gene duplicates and frequent gene conversion. By looking at over 100 fish genomes, our study provides a comprehensive first insight into the *RH2* evolution in fishes. However, we expect future work to resolve many more of the evolutionary intricacies that are hidden away in the genomes of the more than 34,000 teleost species.

FIGURES

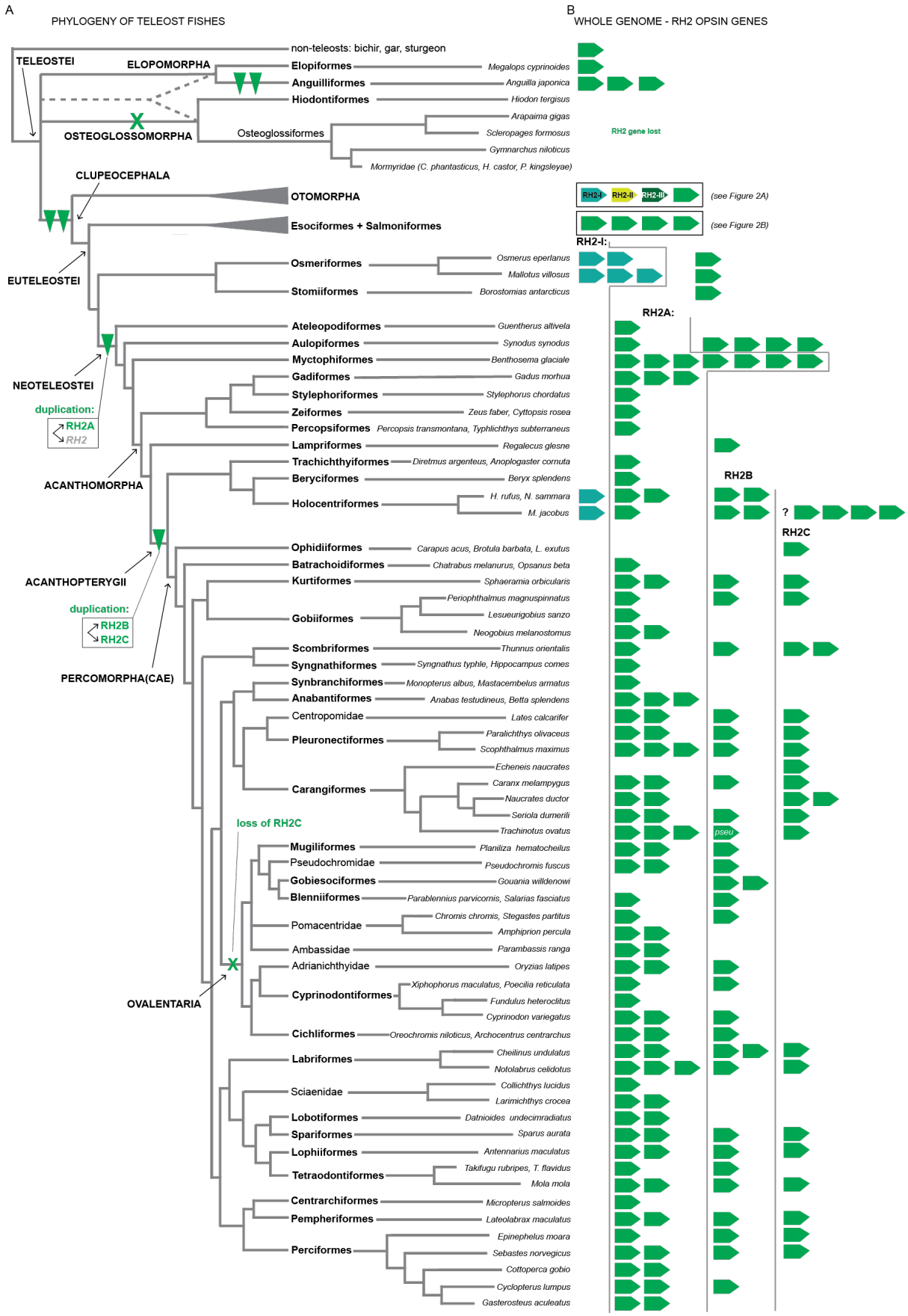
A
PHYLOGENY OF TELEOST FISHES
B
WHOLE GENOME - RH2 OPSIN GENES
non-teleosts: bichir, gar, sturgeon
TELEOSTEI
ELOPOMORPHA
Elopiformes
Megalops cyprinoides
Anguilliformes
Anguilla japonica
Hiodontiformes
Hiodon tergisus
OSTEOGLOSSOMORPHA
Osteoglossiformes
Arapaima gigas
Scleropages formosus
Gymnarchus niloticus
Mormyridae (C. phantasticus, H. castor, P. kingsleyae)
RH2 gene lost
CLUPEOCEPHALA
OTOMORPHA
Esociformes + Salmoniformes
RH2-I
RH2-II
RH2-III
(see Figure 2A)
(see Figure 2B)
EUTELEOSTEI
Osmeriformes
Osmerus eperlanus
Mallotus villosus
Stomiiformes
Borostomias antarcticus
RH2-I:
RH2A:
Ateleopodiformes
Guentherus altivela
Aulopiformes
Synodus synodus
Myctophiformes
Benthosema glaciale
NEOTELEOSTEI
Gadiformes
Gadus morhua
Stylephoriformes
Stylephorus chordatus
duplication:
RH2A
RH2
Zeiformes
Zeus faber, Cyttopsis rosea
Percopsiformes
Percopsis transmontana, Typhlichthys subterraneus
Lampriformes
Regalecus glesne
Trachichthyiformes
Diretmus argenteus, Anoplogaster cornuta
ACANTHOMORPHA
Beryciformes
Beryx splendens
RH2B
Holocentriformes
H. rufus, N. sammara
M. jacobus
?
RH2C
Ophidiiformes
Carapus acus, Brotula barbata, L. exutus
Batrachoidiformes
Chatrabus melanurus, Opsanus beta
ACANTHOPTERYGII
Kurtiformes
Sphaeramia orbicularis
duplication:
RH2B
RH2C
Gobiiformes
Periophthalmus magnuspinnatus
Lesueurigobius sanzo
Neogobius melanostomus
Scombriformes
Thunnus orientalis
Syngnathiformes
Syngnathus typhle, Hippocampus comes
PERCOMORPHA(CAE)
Synbranchiformes
Monopterus albus, Mastacembelus armatus
Anabantiformes
Anabas testudineus, Betta splendens
Centropomidae
Lates calcarifer
Pleuronectiformes
Paralichthys olivaceus
Scophthalmus maximus
Echeneis naucrates
Carangiformes
Caranx melampygus
Naucrates ductor
Seriola dumerili
Trachinotus ovatus
pseu
loss of RH2C
Mugiliformes
Planiliza hematocheilus
Pseudochromidae
Pseudochromis fuscus
Gobiesociformes
Gouania willdenowi
Blenniiformes
Parablennius parvicornis, Salarias fasciatus
Pomacentridae
Chromis chromis, Stegastes partitus
Amphiprion percula
Ambassidae
Parambassis ranga
Adrianichthyidae
Oryzias latipes
OVALENTARIA
Cyprinodontiformes
Xiphophorus maculatus, Poecilia reticulata
Fundulus heteroclitus
Cyprinodon variegatus
Cichliformes
Oreochromis niloticus, Archocentrus centrarchus
Labriformes
Cheilinus undulatus
Notolabrus celidotus
Sciaenidae
Collichthys lucidus
Larimichthys crocea
Lobotiformes
Datnioides undecimradiatus
Spariformes
Sparus aurata
Lophiiformes
Antennarius maculatus
Tetraodontiformes
Takifugu rubripes, T. flavidus
Mola mola
Centrarchiformes
Micropterus salmoides
Pempheriformes
Lateolabrax maculatus
Perciformes
Epinephelus moara
Sebastes norvegicus
Cottoperca gobio
Cyclopterus lumpus
Gasterosteus aculeatus

202 **Figure 1** Evolution and diversity of the *RH2* opsin genes in teleost fishes. A) Schematic
203 phylogeny (after Betancur-R et al., 2017) of the teleost genomes that were analysed in this
204 study. At least two *RH2* gene duplications occurred in the ancestor of Clupeocephala giving
205 rise to the *RH2-I*, *RH2-II*, *RH2-III*, and *RH2* copies. Further duplications occurred later in the
206 ancestor of Neoteleostei (giving rise to *RH2A*) and Acanthopterygii (giving rise to *RH2B* and
207 *RH2C*). Because there is an uncertainty with the assignment of the holocentrid *RH2* genes, the
208 alternative scenario is that this duplication happened in the ancestor of Percomorpha. The *RH2*
209 opsin gene type was lost in Osteoglossomorpha and a few characins (see Escobar-Camacho et
210 al., 2020) for details on characins) the *RH2C* copy was lost in Ovalentaria. B) Number and
211 types of the *RH2* opsins found in the whole genomes of 115 ray-finned fishes. See Fig. 2 for
212 details on the Otomorpha, Esociformes, and Salmoniformes *RH2* evolution. RH2, rhodopsin-
213 like 2 opsin gene; pseu, pseudogene.
214

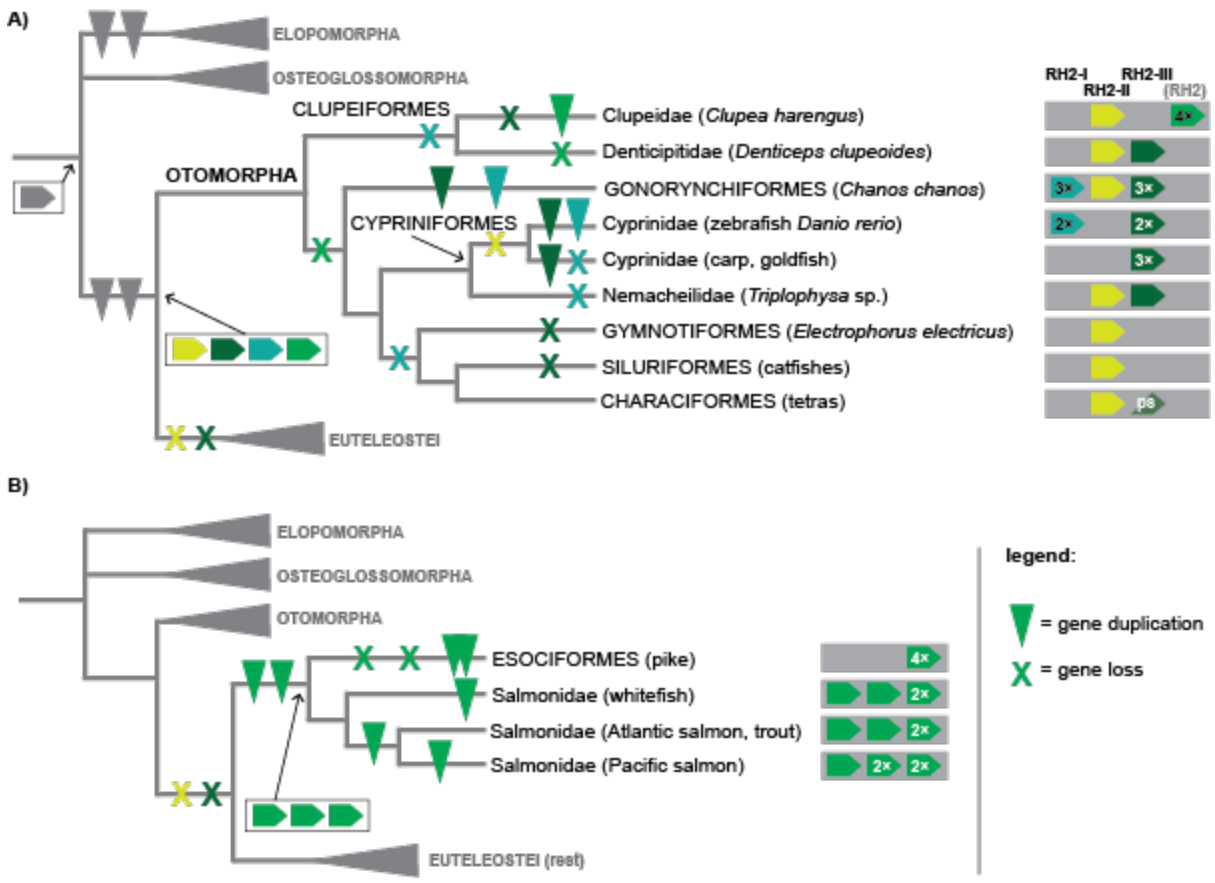

Figure 2 Evolution of the *RH2* opsin genes in Otomorpha, Esociformes, and Salmoniformes. A) In Otomorpha the *RH2* diversity is based on all four ancestral copies. The *RH2-II* and *RH2-III* copies persisted only in Otomorpha, *RH2-I* is also preserved in smelts (Osmeriformes) and soldierfishes (Holocentriformes) (see Fig. 1). The *RH2-I* and *RH2-III* copies are located in the conventional *RH2* cluster flanked by the *synpr* and *slc6A13* genes, similar to the euteleost *RH2s* (data not shown). The *RH2-II* copy is located on the separate cluster next to the *mut5-HS* gene (data not shown). Note, for example, that the only *RH2* gene in catfishes and characins (*RH2-II*) is a different paralog than the copy used in cyprinids (*RH2-III*). B) In pike and salmon, *RH2* duplicated from the fourth ancestral copy, likely in their common ancestor and these paralogs are not shared with other teleost lineages. RH2, rhodopsin-like 2 opsin gene.

227

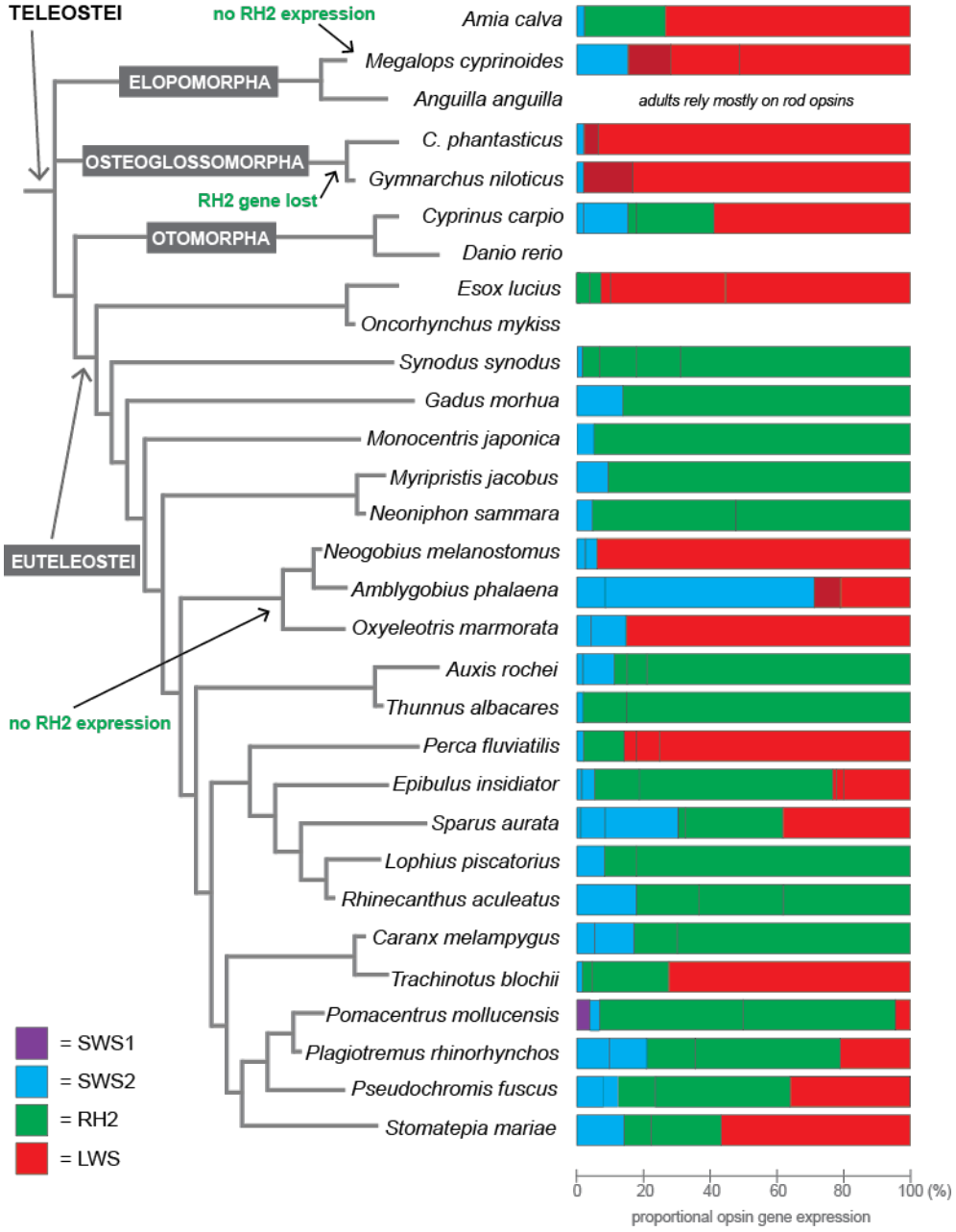

228

229 **Figure 3** Cone opsin gene expression in teleost fishes. The *RH2* opsin gene is expressed in
230 most of the species highlighting its relevance for vision in different aquatic habitats (from deep
231 sea to shallow streams). *RH2* has been lost in Osteoglossmorpha and none or very low *RH2*
232 expression has been observed in tarpon and gobies. In all these fishes, green sensitivity has
233 been taken over by a shorter-wavelength shifted copy of the red sensitive *LWS* opsin (also see
234 Cortesi et al., 2021; Escobar-Camacho et al., 2020; Liu et al., 2018). SWS1 and 2, short-
235 wavelength-sensitive 1 and 2 opsin genes; RH2, rhodopsin-like 2 opsin gene; LWS, long-
236 wavelength-sensitive opsin gene.

237

238 **Material and Methods**

239

240 ***Mining of RH2 opsins from the whole genome dataset***

241 Whole genomic data have been downloaded from GenBank for the species with high-quality
242 genomes. In a few cases, we included lower quality draft genomes if the *RH2* genes were
243 assembled as one cluster or resembling the synteny in high quality genomes. Table S1 contains
244 the details for all species including accession numbers.

245 To search for the *RH2* opsin genes, we have used the following pipeline: assembled
246 genomes have been mapped against the single exons 1 and 4 of the eel (*Anguilla japonica*),
247 blind cavefish (*Astyanax mexicanus*), zebrafish (*Danio rerio*; *RH2-I* and *RH2-III*), pike (*Esox*
248 *lucius*), squirrelfish (*Neoniphon sammara; RH2-I, RH2A* and one uncertain copy) and tilapia
249 (*Oreochromis niloticus*; *RH2Aalpha* and *RH2B*). Mapping was performed in Geneious 9.1.8
250 (www.geneious.com) using the Medium Sensitivity settings. This setting was sensitive enough
251 to make hits on all *RH2* and *RH1* and exo-rhodopsin, the latter two have subsequently been
252 excluded. Scaffolds/chromosomes with positive hits were then screened more in more detail.
253 First, all single exons of all opsin genes from the species mentioned above have been mapped
254 against the scaffold/chromosome with the High Sensitivity settings. This has forced the exons
255 to be mapped in the regions with opsins, and as such served to identify the *RH2* cluster. Once
256 the cluster(s) have been found, we inspected the upstream and downstream region (by mapping
257 again the single exons) to make sure there are no more *RH2* genes in this scaffold. In the *RH2*
258 cluster, we mapped our exons also to every intergenic region (separately), to make sure no gene
259 fragment was overlooked. After extracting the *RH2* genes, we annotated them in Geneious
260 using the "automated annotation" function and the exon/intron boundaries in the annotation
261 were subsequently confirmed via single exon mapping. In those cases, in which annotated
262 genomes were available we used those annotations, but we nevertheless doublechecked the
263 upstream and intergenic regions to exclude the presence of further *RH2* genes.

264

265 ***Phylogenetic analysis***

266 The final dataset contained 417 *RH2* sequences (plus one exo-rhodopsin outgroup). All *RH2*
267 sequences were aligned using the MAFFT plug-in as implemented in Geneious v.9.1.8 (Katoh
268 et al., 2019). Due to the uncertainties with the identity and annotation of exon 5 (shorter than
269 other exons), we have excluded this exon from the alignment. We have reconstructed the *RH2*
270 gene tree using the MrBayes 3.2 (Ronquist et al., 2012) software on the CIPRES portal (Miller
271 et al., 2010). MrBayes was run four times independently (each with two runs) with 50 million

generations each. We the visually inspected the resulting output files in Tracer 1.5 (https://beast.community/) to identify the run with the best -lnL score and the number of generations it took for each run to reach the -lnL plateau. Four out of the eight resulting files were selected, and a consensus tree reconstructed using a burnin of 25 million generations.

Transcriptome analysis

Transcriptomic reads were mapped against a general reference including all known rod and cone opsin gene types (references from: tilapia, zebrafish, Round goby, cavefish) with Medium Sensitivity settings in Geneious 9.1.8. If only one copy per type was found in a given species, the consensus was exported and used as a species-specific reference. If multiple copies per opsin type were present, we manually disentangled the copies (for details methods see de Busserolles et al., 2017 and Musilova et al., 2019). The transcriptomic reads were then mapped again against each species-specific reference dataset with the Lowest Sensitivity settings. The number of reads that mapped to each copy were then used to calculate the proportion (in %) of expression of each opsin type from the total cone opsin expression as per de Busserolles et al., 2017 and Tettamanti et al., 2019.

Acknowledgement

We would also like to acknowledge the indigenous owners of the land on which some of the reported research has been carried out or from which specimens reported in this study derive. FC was supported by an Australian Research Council DECRA Research Fellowship (ARC DE200100620) and a University of Queensland Development Fellowship. ZM was supported by the Swiss National Science Foundation (SNF grant PROMYS, 166550), Charles University (Primus), and the Czech Science Foundation (21-31712S).

References

Betancur-R, R., Wiley, E. O., Arratia, G., Acero, A., Bailly, N., Miya, M., Lecointre, G. and Ortí, G. (2017). Phylogenetic classification of bony fishes. *BMC Evol. Biol.* **17**, 162.

Busserolles, F. de, Cortesi, F., Fogg, L., Stieb, S. M., Luehrmann, M. and Marshall, N. J. (2021). The visual ecology of Holocentridae, a nocturnal coral reef fish family with a deep-sea-like multibank retina. *J. Exp. Biol.* **224**,.

Carleton, K. L. and Yourick, M. R. (2020). Axes of visual adaptation in the ecologically diverse family Cichlidae. *Semin. Cell Dev. Biol.*

Carleton, K. L., Escobar-Camacho, D., Stieb, S. M., Cortesi, F. and Marshall, N. J. (2020). Seeing the rainbow: mechanisms underlying spectral sensitivity in teleost fishes. *J. Exp. Biol.* **223**,.

Carvalho, L. S., Pessoa, D. M. A., Mountford, J. K., Davies, W. I. L. and Hunt, D. M. (2017). The Genetic and Evolutionary Drives behind Primate Color Vision. *Front. Ecol. Evol.* **5**,.

Chang, C.-H., Catchen, J., Moran, R. L., Rivera-Colón, A. G., Wang, Y.-C. and Fuller, R. C. (2021). Sequence analysis and ontogenetic expression patterns of cone opsin genes in the bluefin killifish (Lucania goodei). *J. Hered.*

Chen, J.-N., Samadi, S. and Chen, W.-J. (2018). Rhodopsin gene evolution in early teleost fishes. *PLoS ONE* **13**, e0206918.

Cortesi, F., Musilová, Z., Stieb, S. M., Hart, N. S., Siebeck, U. E., Malmstrøm, M., Tørresen, O. K., Jentoft, S., Cheney, K. L., Marshall, N. J., et al. (2015). Ancestral duplications and highly dynamic opsin gene evolution in percomorph fishes. *Proc. Natl. Acad. Sci.* **112**, 1493–1498.

Cortesi, F., Musilová, Z., Stieb, S. M., Hart, N. S., Siebeck, U. E., Cheney, K. L., Salzburger, W. and Marshall, N. J. (2016). From crypsis to mimicry: changes in colour and the configuration of the visual system during ontogenetic habitat transitions in a coral reef fish. *J. Exp. Biol.* **219**, 2545–2558.

Cortesi, F., Camacho, D. E., Luehrmann, M., Sommer, G. M. and Musilova, Z. (2021). Multiple ancestral duplications of the red-sensitive opsin gene (LWS) in teleost fishes and convergent spectral shifts to green vision in gobies. *bioRxiv* 2021.05.08.443214.

de Busserolles, F., Cortesi, F., Helvik, J. V., Davies, W. I., Templin, R. M., Sullivan, R. K., Michell, C. T., Mountford, J. K., Collin, S. P. and Irigoien, X. (2017). Pushing the limits of photoreception in twilight conditions: The rod-like cone retina of the deep-sea pearlsides. *Sci. Adv.* **3**, eaao4709.

Escobar-Camacho, D., Ramos, E., Martins, C. and Carleton, K. L. (2017). The Opsin Genes of Amazonian Cichlids. *Mol. Ecol.* **26**, 1343–1356.

Escobar-Camacho, D., Carleton, K. L., Narain, D. W. and Pierotti, M. E. R. (2020). Visual pigment evolution in Characiformes: the dynamic interplay of teleost whole-genome duplication, surviving opsins and spectral tuning. *Mol. Ecol.* **n/a**,.

Giske, J., Aksnes, D. L., Baliño, B. M., Kaartvedt, S., Lie, U., Nordeide, J. T., Salvanes, A. G. V., Wakili, S. M. and Aadnesen, A. (1990). Vertical distribution and trophic interactions of zooplankton and fish in Masfjorden, Norway. *Sarsia* **75**, 65–81.

Hunt, D. M., Hankins, M. W., Collin, S. P. and Marshall, N. J. (2014). *Evolution of visual and non-visual pigments*. Springer.

Jerlov, N. G. (1976). *Marine Optics*. Amsterdam: Elsevier.

Katoh, K., Rozewicki, J. and Yamada, K. D. (2019). MAFFT online service: multiple sequence alignment, interactive sequence choice and visualization. *Brief. Bioinform.* **20**, 1160–1166.

Lamb, T. D. (2013). Evolution of phototransduction, vertebrate photoreceptors and retina. *Prog. Retin. Eye Res.* **36**, 52–119.

Lien, S., Koop, B. F., Sandve, S. R., Miller, J. R., Kent, M. P., Nome, T., Hvidsten, T. R.,

Leong, J. S., Minkley, D. R., Zimin, A., et al. (2016). The Atlantic salmon genome provides insights into rediploidization. *Nature* **533**, 200–205.

Lin, J.-J., Wang, F.-Y., Li, W.-H. and Wang, T.-Y. (2017). The rises and falls of opsin genes in 59 ray-finned fish genomes and their implications for environmental adaptation. *Sci. Rep.* **7**, 15568.

Liu, D. W., Wang, F. Y., Lin, J. J., Thompson, A., Lu, Y., Vo, D., Yan, H. Y. and Zakon, H. (2018). The cone opsin repertoire of osteoglossomorph fishes: gene loss in mormyrid electric fish and a long wave-length sensitive cone opsin that survived 3R. *Mol Biol Evol*.

Luehrmann, M., Carleton, K. L., Cortesi, F., Cheney, K. L. and Marshall, N. J. (2019). Cardinalfishes (Apogonidae) show visual system adaptations typical of nocturnally and diurnally active fish. *Mol. Ecol.* **28**, 3025–3041.

Lupše, N., Cortesi, F., Freese, M., Marohn, L., Pohlman, J.-D., Wysujack, K., Hanel, R. and Musilova, Z. (2021). The expression of deep-sea fish visual genes supports a conserved cone-to-rod vertebrate retinal development. *bioRxiv* 2020.05.25.114991.

Matsumoto, Y., Oda, S., Mitani, H. and Kawamura, S. (2020). Orthologous divergence and paralogous anti-convergence in molecular evolution of triplicated green opsin genes in medaka fish, genus Oryzias. *Genome Biol. Evol.* evaa111.

Miller, M. A., Pfeiffer, W. and Schwartz, T. (2010). Creating the CIPRES Science Gateway for inference of large phylogenetic trees.pp. 1–8. IEEE.

Munz, F. W. and McFarland, W. N. (1977). Evolutionary adaptations of fishes to the photic environment. In *The Visual System in Vertebrates* (ed. Crescitelli, F.), Dvorak, C. A.), Eder, D. J.), Granda, A. M.), Hamasaki, D.), Holmberg, K.), Hughes, A.), Locket, N. A.), McFarland, W. N.), Meyer, D. B.), et al.), pp. 193–274. Berlin, Heidelberg: Springer.

Musilova, Z., Cortesi, F., Matschiner, M., Davies, W. I. L., Patel, J. S., Stieb, S. M., Busserolles, F. de, Malmstrøm, M., Tørresen, O. K., Brown, C. J., et al. (2019). Vision using multiple distinct rod opsins in deep-sea fishes. *Science* **364**, 588–592.

Musilova, Z., Salzburger, W. and Cortesi, F. (2021). The visual opsin gene repertoires of teleost fishes: evolution, ecology, and funtion. *Press*.

Rennison, D. J., Owens, G. L. and Taylor, J. S. (2012). Opsin gene duplication and divergence in ray-finned fish. *Mol. Phylogenet. Evol.* **62**, 986–1008.

Rhie, A., McCarthy, S. A., Fedrigo, O., Damas, J., Formenti, G., Koren, S., Uliano-Silva, M., Chow, W., Fungtammasan, A., Kim, J., et al. (2021). Towards complete and error-free genome assemblies of all vertebrate species. *Nature* **592**, 737–746.

Ronquist, F., Teslenko, M., van der Mark, P., Ayres, D. L., Darling, A., Höhna, S., Larget, B., Liu, L., Suchard, M. A. and Huelsenbeck, J. P. (2012). MrBayes 3.2: efficient Bayesian phylogenetic inference and model choice across a large model space. *Syst. Biol.* **61**, 539–542.

Sandkam, B. A., Joy, J. B., Watson, C. T. and Breden, F. (2017). Genomic Environment Impacts Color Vision Evolution in a Family with Visually Based Sexual Selection. *Genome Biol. Evol.* **9**, 3100–3107.

Tettamanti, V., Busserolles, F. de, Lecchini, D., Marshall, N. J. and Cortesi, F. (2019). Visual system development of the spotted unicornfish, *Naso brevirostris* (Acanthuridae). *J. Exp. Biol.* **222**,.

Wald, G. (1968). The molecular basis of visual excitation. *Nature* **219**, 800.

Yokoyama, S. (2008). Evolution of dim-light and color vision pigments. *Annu Rev Genomics Hum Genet* **9**, 259–282.

Yokoyama, S. and Jia, H. (2020). Origin and adaptation of green-sensitive (RH2) pigments in vertebrates. *FEBS Open Bio* **n/a**,.

Yokoyama, R. and Yokoyama, S. (1990). Convergent evolution of the red- and green-like visual pigment genes in fish, Astyanax fasciatus, and human. *Proc. Natl. Acad. Sci.* **87**, 9315–9318.

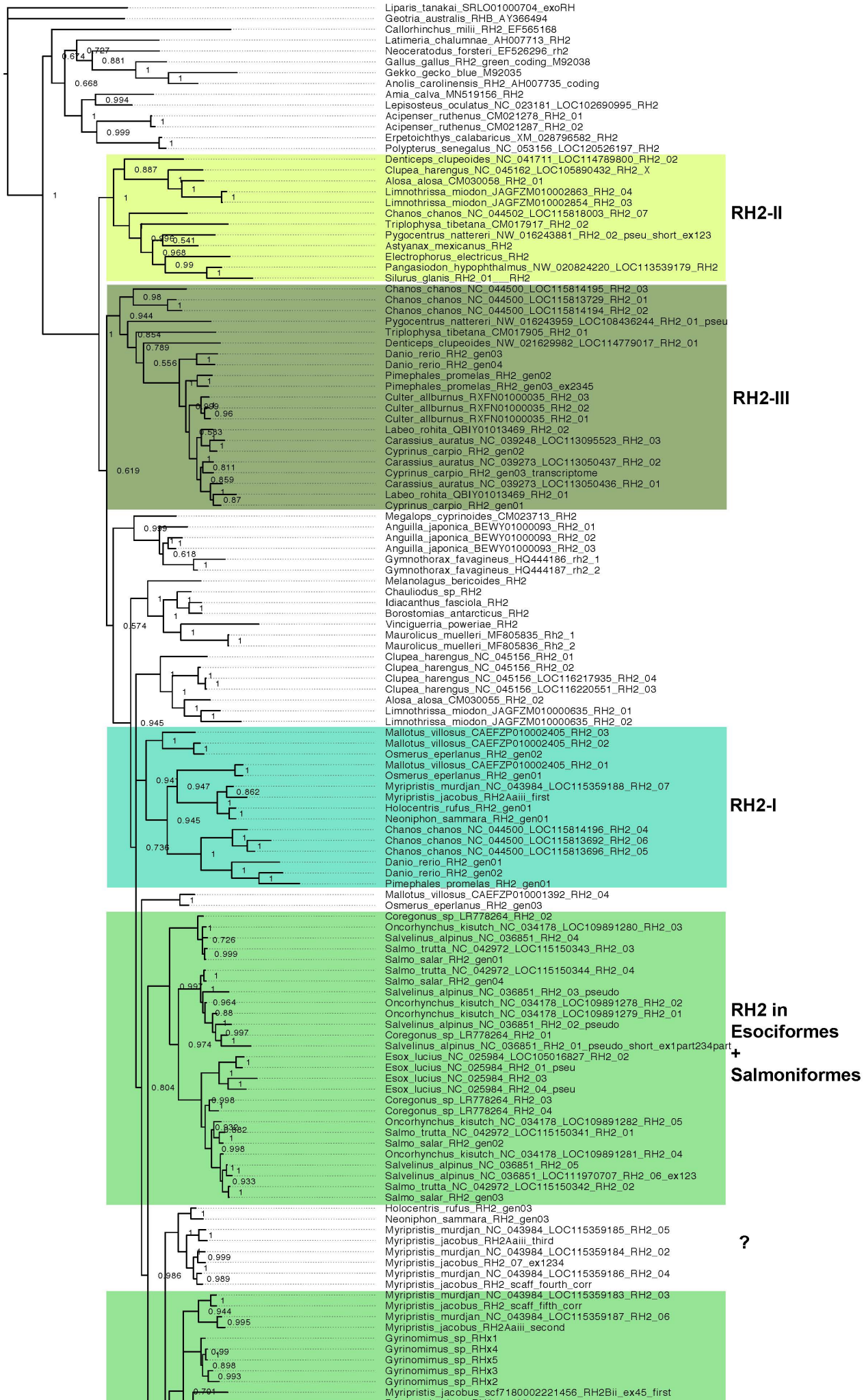
Liparis_tanakai_SRLO01000704_exoRH
Geotria_australis_RHB_AY366494
Callorhinchus_milii_RH2_EF565168
Latimeria_chalumnae_AH007713_RH2
Neoceratodus_forsteri_EF526296_rh2
Gallus_gallus_RH2_green_coding_M92038
Gekko_gecko_blue_M92035
Anolis_carolinensis_RH2_AH007735_coding
Amia_calva_MN519156_RH2
Lepisosteus_oculatus_NC_023181_LOC102690995_RH2
Acipenser_ruthenus_CM021278_RH2_01
Acipenser_ruthenus_CM021287_RH2_02
Erpetoichthys_calabaricus_XM_028796582_RH2
Polypterus_senegalus_NC_053156_LOC120526197_RH2
Denticeps_clupeoides_NC_041711_LOC114789800_RH2_02
Clupea_harengus_NC_045162_LOC105890432_RH2_X
Alosa_alosa_CM030058_RH2_01
Limnothrissa_miodon_JAGFZM010002863_RH2_04
Limnothrissa_miodon_JAGFZM010002854_RH2_03
Chanos_chanos_NC_044502_LOC115818003_RH2_07
Triplophysa_tibetana_CM017917_RH2_02
Pygocentrus_nattereri_NW_016243881_RH2_02_pseu_short_ex123
Astyanax_mexicanus_RH2
Electrophorus_electricus_RH2
Pangasiodon_hypophthalmus_NW_020824220_LOC113539179_RH2
Silurus_glanis_RH2_01___RH2
RH2-II
Chanos_chanos_NC_044500_LOC115814195_RH2_03
Chanos_chanos_NC_044500_LOC115813729_RH2_01
Chanos_chanos_NC_044500_LOC115814194_RH2_02
Pygocentrus_nattereri_NW_016243959_LOC108436244_RH2_01_pseu
Triplophysa_tibetana_CM017905_RH2_01
Denticeps_clupeoides_NW_021629982_LOC114779017_RH2_01
Danio_rerio_RH2_gen03
Danio_rerio_RH2_gen04
Pimephales_promelas_RH2_gen02
Pimephales_promelas_RH2_gen03_ex2345
Culter_allburnus_RXFN01000035_RH2_03
Culter_allburnus_RXFN01000035_RH2_02
Culter_allburnus_RXFN01000035_RH2_01
Labeo_rohita_QBIY01013469_RH2_02
Carassius_auratus_NC_039248_LOC113095523_RH2_03
Cyprinus_carpio_RH2_gen02
Carassius_auratus_NC_039273_LOC113050437_RH2_02
Cyprinus_carpio_RH2_gen03_transcriptome
Carassius_auratus_NC_039273_LOC113050436_RH2_01
Labeo_rohita_QBIY01013469_RH2_01
Cyprinus_carpio_RH2_gen01
RH2-III
Megalops_cyprinoides_CM023713_RH2
Anguilla_japonica_BEWY01000093_RH2_01
Anguilla_japonica_BEWY01000093_RH2_02
Anguilla_japonica_BEWY01000093_RH2_03
Gymnothorax_favagineus_HQ444186_rh2_1
Gymnothorax_favagineus_HQ444187_rh2_2
Melanolagus_bericoides_RH2
Chauliodus_sp_RH2
Idiacanthus_fasciola_RH2
Borostomias_antarcticus_RH2
Vinciguerria_poweriae_RH2
Maurolicus_muelleri_MF805835_Rh2_1
Maurolicus_muelleri_MF805836_Rh2_2
Clupea_harengus_NC_045156_RH2_01
Clupea_harengus_NC_045156_RH2_02
Clupea_harengus_NC_045156_LOC116217935_RH2_04
Clupea_harengus_NC_045156_LOC116220551_RH2_03
Alosa_alosa_CM030055_RH2_02
Limnothrissa_miodon_JAGFZM010000635_RH2_01
Limnothrissa_miodon_JAGFZM010000635_RH2_02
Mallotus_villosus_CAEFZP010002405_RH2_03
Mallotus_villosus_CAEFZP010002405_RH2_02
Osmerus_eperlanus_RH2_gen02
Mallotus_villosus_CAEFZP010002405_RH2_01
Osmerus_eperlanus_RH2_gen01
Myripristis_murdjan_NC_043984_LOC115359188_RH2_07
Myripristis_jacobus_RH2Aaiii_first
Holocentris_rufus_RH2_gen01
Neoniphon_sammara_RH2_gen01
Chanos_chanos_NC_044500_LOC115814196_RH2_04
Chanos_chanos_NC_044500_LOC115813692_RH2_06
Chanos_chanos_NC_044500_LOC115813696_RH2_05
Danio_rerio_RH2_gen01
Danio_rerio_RH2_gen02
Pimephales_promelas_RH2_gen01
RH2-I
Mallotus_villosus_CAEFZP010001392_RH2_04
Osmerus_eperlanus_RH2_gen03
Coregonus_sp_LR778264_RH2_02
Oncorhynchus_kisutch_NC_034178_LOC109891280_RH2_03
Salvelinus_alpinus_NC_036851_RH2_04
Salmo_trutta_NC_042972_LOC115150343_RH2_03
Salmo_salar_RH2_gen01
Salmo_trutta_NC_042972_LOC115150344_RH2_04
Salmo_salar_RH2_gen04
Salvelinus_alpinus_NC_036851_RH2_03_pseudo
Oncorhynchus_kisutch_NC_034178_LOC109891278_RH2_02
Oncorhynchus_kisutch_NC_034178_LOC109891279_RH2_01
Salvelinus_alpinus_NC_036851_RH2_02_pseudo
Coregonus_sp_LR778264_RH2_01
Salvelinus_alpinus_NC_036851_RH2_01_pseudo_short_ex1part234part
Esox_lucius_NC_025984_LOC105016827_RH2_02
Esox_lucius_NC_025984_RH2_01_pseu
Esox_lucius_NC_025984_RH2_03
Esox_lucius_NC_025984_RH2_04_pseu
Coregonus_sp_LR778264_RH2_03
Coregonus_sp_LR778264_RH2_04
Oncorhynchus_kisutch_NC_034178_LOC109891282_RH2_05
Salmo_trutta_NC_042972_LOC115150341_RH2_01
Salmo_salar_RH2_gen02
Oncorhynchus_kisutch_NC_034178_LOC109891281_RH2_04
Salvelinus_alpinus_NC_036851_RH2_05
Salvelinus_alpinus_NC_036851_LOC111970707_RH2_06_ex123
Salmo_trutta_NC_042972_LOC115150342_RH2_02
Salmo_salar_RH2_gen03
RH2 in Esociformes + Salmoniformes
Holocentris_rufus_RH2_gen03
Neoniphon_sammara_RH2_gen03
Myripristis_murdjan_NC_043984_LOC115359185_RH2_05
Myripristis_jacobus_RH2Aaiii_third
Myripristis_murdjan_NC_043984_LOC115359184_RH2_02
Myripristis_jacobus_RH2_07_ex1234
Myripristis_murdjan_NC_043984_LOC115359186_RH2_04
Myripristis_jacobus_RH2_scaff_fourth_corr
Myripristis_murdjan_NC_043984_LOC115359183_RH2_03
Myripristis_jacobus_RH2_scaff_fifth_corr
Myripristis_murdjan_NC_043984_LOC115359187_RH2_06
Myripristis_jacobus_RH2Aaiii_second
Gyrinomimus_sp_RHx1
Gyrinomimus_sp_RHx4
Gyrinomimus_sp_RHx5
Gyrinomimus_sp_RHx3
Gyrinomimus_sp_RHx2
Myripristis_jacobus_scf7180002221456_RH2Bii_ex45_first
?

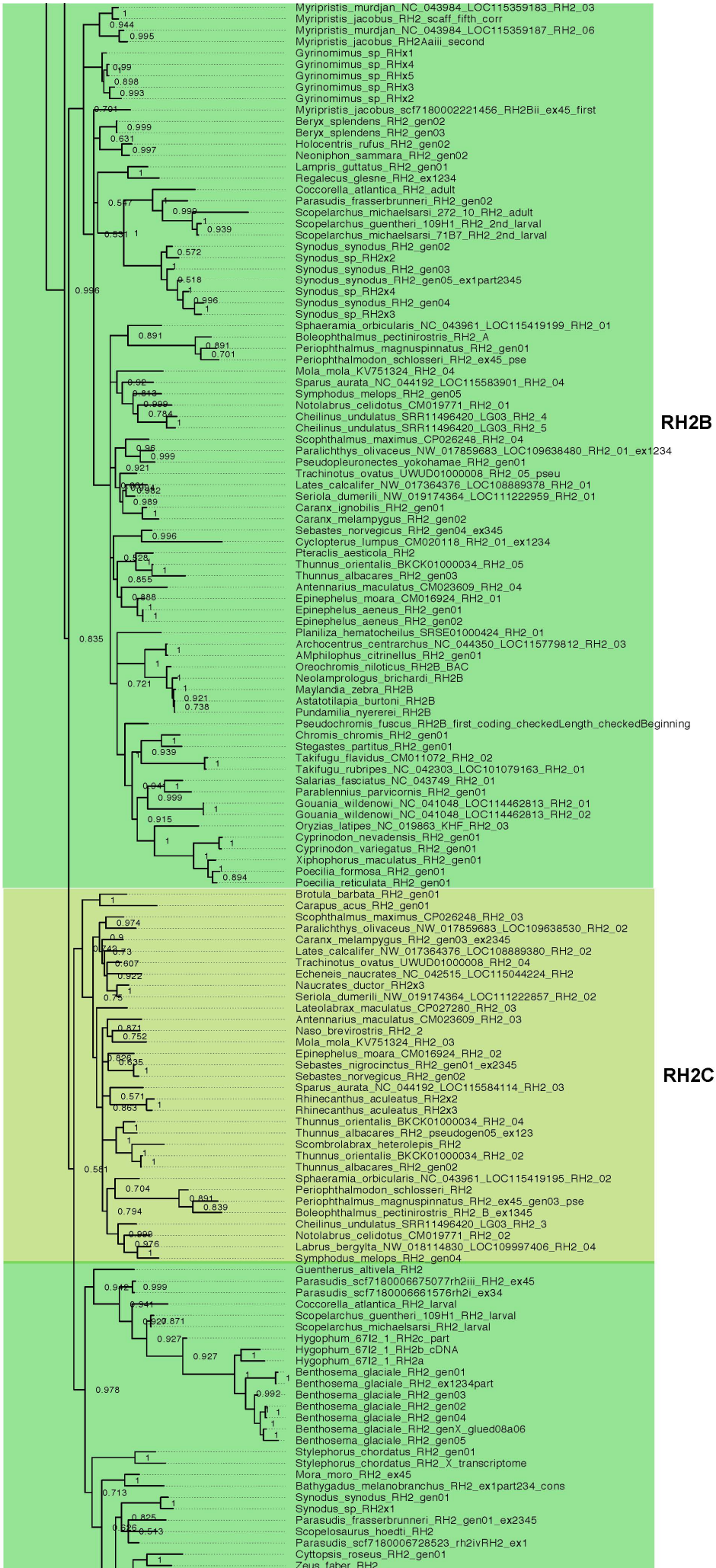
Myripristis_murdjan_NC_043984_LOC115359183_RH2_03
Myripristis_jacobus_RH2_scaff_fifth_corr
Myripristis_murdjan_NC_043984_LOC115359187_RH2_06
Myripristis_jacobus_RH2Aaiii_second
Gyrinomimus_sp_RHx1
Gyrinomimus_sp_RHx4
Gyrinomimus_sp_RHx5
Gyrinomimus_sp_RHx3
Gyrinomimus_sp_RHx2
Myripristis_jacobus_scf7180002221456_RH2Bii_ex45_first
Beryx_splendens_RH2_gen02
Beryx_splendens_RH2_gen03
Holocentris_rufus_RH2_gen02
Neoniphon_sammara_RH2_gen02
Lampris_guttatus_RH2_gen01
Regalecus_glesne_RH2_ex1234
Coccorella_atlantica_RH2_adult
Parasudis_frasserbrunneri_RH2_gen02
Scopelarchus_michaelsarsi_272_10_RH2_adult
Scopelarchus_guentheri_109H1_RH2_2nd_larval
Scopelarchus_michaelsarsi_71B7_RH2_2nd_larval
Synodus_synodus_RH2_gen02
Synodus_sp_RH2x2
Synodus_synodus_RH2_gen03
Synodus_synodus_RH2_gen05_ex1part2345
Synodus_sp_RH2x4
Synodus_synodus_RH2_gen04
Synodus_sp_RH2x3
Sphaeramia_orbicularis_NC_043961_LOC115419199_RH2_01
Boleophthalmus_pectinirostris_RH2_A
Periophthalmus_magnuspinnatus_RH2_gen01
Periophthalmodon_schlosseri_RH2_ex45_pse
Mola_mola_KV751324_RH2_04
Sparus_aurata_NC_044192_LOC115583901_RH2_04
Symphodus_melops_RH2_gen05
Notolabrus_celidotus_CM019771_RH2_01
Cheilinus_undulatus_SRR11496420_LG03_RH2_4
Cheilinus_undulatus_SRR11496420_LG03_RH2_5
Scophthalmus_maximus_CP026248_RH2_04
Paralichthys_olivaceus_NW_017859683_LOC109638480_RH2_01_ex1234
Pseudopleuronectes_yokohamae_RH2_gen01
Trachinotus_ovatus_UWUD01000008_RH2_05_pseu
Lates_calcalifer_NW_017364376_LOC108889378_RH2_01
Seriola_dumerili_NW_019174364_LOC111222959_RH2_01
Caranx_ignobilis_RH2_gen01
Caranx_melampygus_RH2_gen02
Sebastes_norvegicus_RH2_gen04_ex345
Cyclopterus_lumpus_CM020118_RH2_01_ex1234
Pteraclis_aesticola_RH2
Thunnus_orientalis_BKCK01000034_RH2_05
Thunnus_albacares_RH2_gen03
Antennarius_maculatus_CM023609_RH2_04
Epinephelus_moara_CM016924_RH2_01
Epinephelus_aeneus_RH2_gen01
Epinephelus_aeneus_RH2_gen02
Planiliza_hematocheilus_SRSE01000424_RH2_01
Archocentrus_centrarchus_NC_044350_LOC115779812_RH2_03
AMphilophus_citrinellus_RH2_gen01
Oreochromis_niloticus_RH2B_BAC
Neolamprologus_brichardi_RH2B
Maylandia_zebra_RH2B
Astatotilapia_burtoni_RH2B
Pundamilia_nyererei_RH2B
Pseudochromis_fuscus_RH2B_first_coding_checkedLength_checkedBeginning
Chromis_chromis_RH2_gen01
Stegastes_partitus_RH2_gen01
Takifugu_flavidus_CM011072_RH2_02
Takifugu_rubripes_NC_042303_LOC101079163_RH2_01
Salarias_fasciatus_NC_043749_RH2_01
Parablennius_parvicornis_RH2_gen01
Gouania_wildenowi_NC_041048_LOC114462813_RH2_01
Gouania_wildenowi_NC_041048_LOC114462813_RH2_02
Oryzias_latipes_NC_019863_KHF_RH2_03
Cyprinodon_nevadensis_RH2_gen01
Cyprinodon_variegatus_RH2_gen01
Xiphophorus_maculatus_RH2_gen01
Poecilia_formosa_RH2_gen01
Poecilia_reticulata_RH2_gen01
RH2B
Brotula_barbata_RH2_gen01
Carapus_acus_RH2_gen01
Scophthalmus_maximus_CP026248_RH2_03
Paralichthys_olivaceus_NW_017859683_LOC109638530_RH2_02
Caranx_melampygus_RH2_gen03_ex2345
Lates_calcalifer_NW_017364376_LOC108889380_RH2_02
Trachinotus_ovatus_UWUD01000008_RH2_04
Echeneis_naucrates_NC_042515_LOC115044224_RH2
Naucrates_ductor_RH2x3
Seriola_dumerili_NW_019174364_LOC111222857_RH2_02
Lateolabrax_maculatus_CP027280_RH2_03
Antennarius_maculatus_CM023609_RH2_03
Naso_brevirostris_RH2_2
Mola_mola_KV751324_RH2_03
Epinephelus_moara_CM016924_RH2_02
Sebastes_nigrocinctus_RH2_gen01_ex2345
Sebastes_norvegicus_RH2_gen02
Sparus_aurata_NC_044192_LOC115584114_RH2_03
Rhinecanthus_aculeatus_RH2x2
Rhinecanthus_aculeatus_RH2x3
Thunnus_orientalis_BKCK01000034_RH2_04
Thunnus_albacares_RH2_pseudogen05_ex123
Scombrolabrax_heterolepis_RH2
Thunnus_orientalis_BKCK01000034_RH2_02
Thunnus_albacares_RH2_gen02
Sphaeramia_orbicularis_NC_043961_LOC115419195_RH2_02
Periophthalmodon_schlosseri_RH2
Periophthalmus_magnuspinnatus_RH2_ex45_gen03_pse
Boleophthalmus_pectinirostris_RH2_B_ex1345
Cheilinus_undulatus_SRR11496420_LG03_RH2_3
Notolabrus_celidotus_CM019771_RH2_02
Labrus_bergylta_NW_018114830_LOC109997406_RH2_04
Symphodus_melops_RH2_gen04
RH2C
Guentherus_altivela_RH2
Parasudis_scf7180006675077rh2iii_RH2_ex45
Parasudis_scf7180006661576rh2i_ex34
Coccorella_atlantica_RH2_larval
Scopelarchus_guentheri_109H1_RH2_larval
Scopelarchus_michaelsarsi_RH2_larval
Hygophum_67I2_1_RH2c_part
Hygophum_67I2_1_RH2b_cDNA
Hygophum_67I2_1_RH2a
Benthosema_glaciale_RH2_gen01
Benthosema_glaciale_RH2_ex1234part
Benthosema_glaciale_RH2_gen03
Benthosema_glaciale_RH2_gen02
Benthosema_glaciale_RH2_gen04
Benthosema_glaciale_RH2_genX_glued08a06
Benthosema_glaciale_RH2_gen05
Stylephorus_chordatus_RH2_gen01
Stylephorus_chordatus_RH2_X_transcriptome
Mora_moro_RH2_ex45
Bathygadus_melanobranchus_RH2_ex1part234_cons
Synodus_synodus_RH2_gen01
Synodus_sp_RH2x1
Parasudis_frasserbrunneri_RH2_gen01_ex2345
Scopelosaurus_hoedti_RH2
Parasudis_scf7180006728523_rh2ivRH2_ex1
Cyttopsis_roseus_RH2_gen01
Zeus_faber_RH2

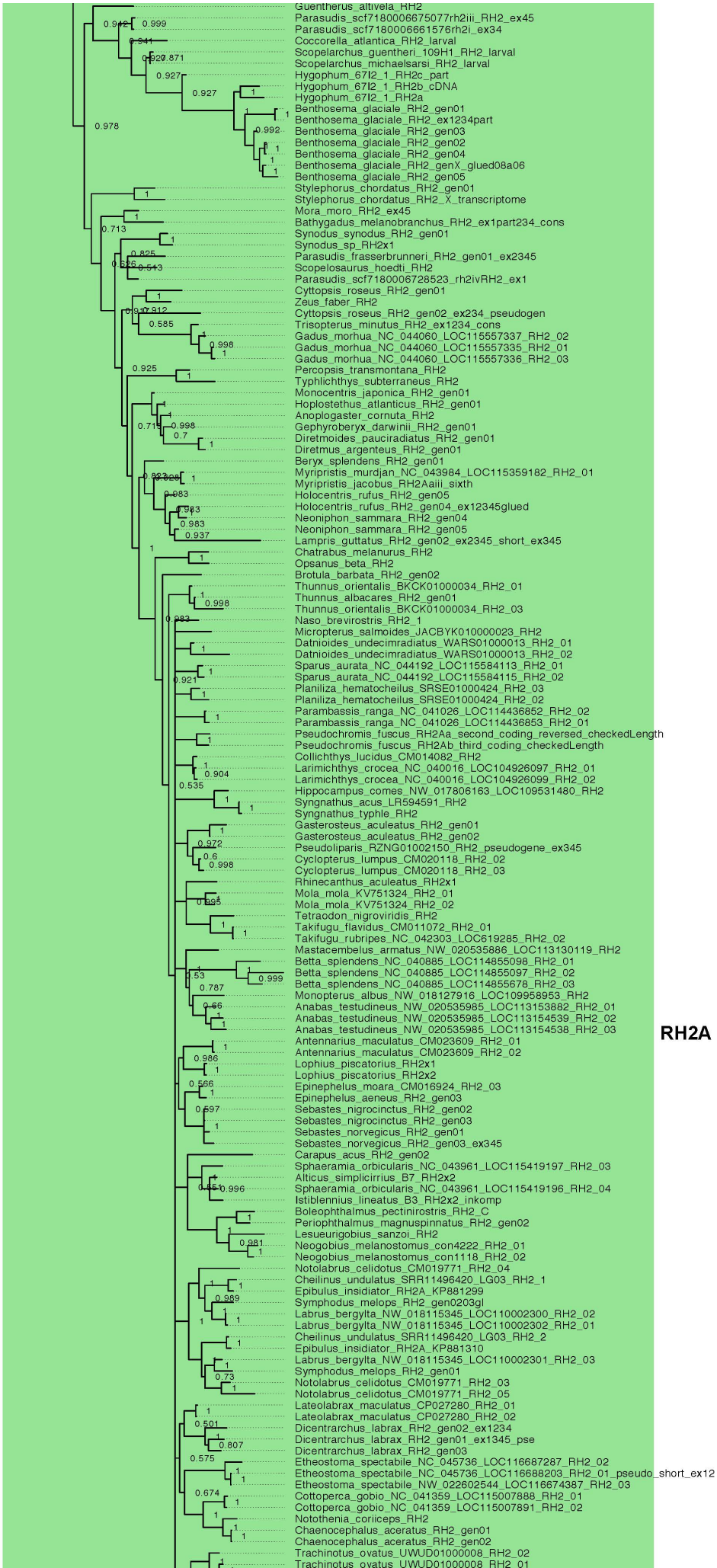
Guentherus_altivela_RH2
Parasudis_scf7180006675077rh2iii_RH2_ex45
Parasudis_scf7180006661576rh2i_ex34
Coccorella_atlantica_RH2_larval
Scopelarchus_guentheri_109H1_RH2_larval
Scopelarchus_michaelsarsi_RH2_larval
Hygophum_67I2_1_RH2c_part
Hygophum_67I2_1_RH2b_cDNA
Hygophum_67I2_1_RH2a
Benthosema_glaciale_RH2_gen01
Benthosema_glaciale_RH2_ex1234part
Benthosema_glaciale_RH2_gen03
Benthosema_glaciale_RH2_gen02
Benthosema_glaciale_RH2_gen04
Benthosema_glaciale_RH2_genX_glued08a06
Benthosema_glaciale_RH2_gen05
Stylephorus_chordatus_RH2_gen01
Stylephorus_chordatus_RH2_X_transcriptome
Mora_moro_RH2_ex45
Bathygadus_melanobranchus_RH2_ex1part234_cons
Synodus_synodus_RH2_gen01
Synodus_sp_RH2x1
Parasudis_frasserbrunneri_RH2_gen01_ex2345
Scopelosaurus_hoedti_RH2
Parasudis_scf7180006728523_rh2ivRH2_ex1
Cyttopsis_roseus_RH2_gen01
Zeus_faber_RH2
Cyttopsis_roseus_RH2_gen02_ex234_pseudogen
Trisopterus_minutus_RH2_ex1234_cons
Gadus_morhua_NC_044060_LOC115557337_RH2_02
Gadus_morhua_NC_044060_LOC115557335_RH2_01
Gadus_morhua_NC_044060_LOC115557336_RH2_03
Percopsis_transmontana_RH2
Typhlichthys_subterraneus_RH2
Monocentris_japonica_RH2_gen01
Hoplostethus_atlanticus_RH2_gen01
Anoplogaster_cornuta_RH2
Gephyroberyx_darwinii_RH2_gen01
Diretmoides_pauciradiatus_RH2_gen01
Diretmus_argenteus_RH2_gen01
Beryx_splendens_RH2_gen01
Myripristis_murdjan_NC_043984_LOC115359182_RH2_01
Myripristis_jacobus_RH2Aaiii_sixth
Holocentris_rufus_RH2_gen05
Holocentris_rufus_RH2_gen04_ex12345glued
Neoniphon_sammara_RH2_gen04
Neoniphon_sammara_RH2_gen05
Lampris_guttatus_RH2_gen02_ex2345_short_ex345
Chatrabus_melanurus_RH2
Opsanus_beta_RH2
Brotula_barbata_RH2_gen02
Thunnus_orientalis_BKCK01000034_RH2_01
Thunnus_albacares_RH2_gen01
Thunnus_orientalis_BKCK01000034_RH2_03
Naso_brevirostris_RH2_1
Micropterus_salmoides_JACBYK010000023_RH2
Datnioides_undecimradiatus_WARS01000013_RH2_01
Datnioides_undecimradiatus_WARS01000013_RH2_02
Sparus_aurata_NC_044192_LOC115584113_RH2_01
Sparus_aurata_NC_044192_LOC115584115_RH2_02
Planiliza_hematocheilus_SRSE01000424_RH2_03
Planiliza_hematocheilus_SRSE01000424_RH2_02
Parambassis_ranga_NC_041026_LOC114436852_RH2_02
Parambassis_ranga_NC_041026_LOC114436853_RH2_01
Pseudochromis_fuscus_RH2Aa_second_coding_reversed_checkedLength
Pseudochromis_fuscus_RH2Ab_third_coding_checkedLength
Collichthys_lucidus_CM014082_RH2
Larimichthys_crocea_NC_040016_LOC104926097_RH2_01
Larimichthys_crocea_NC_040016_LOC104926099_RH2_02
Hippocampus_comes_NW_017806163_LOC109531480_RH2
Syngnathus_acus_LR594591_RH2
Syngnathus_typhle_RH2
Gasterosteus_aculeatus_RH2_gen01
Gasterosteus_aculeatus_RH2_gen02
Pseudoliparis_RZNG01002150_RH2_pseudogene_ex345
Cyclopterus_lumpus_CM020118_RH2_02
Cyclopterus_lumpus_CM020118_RH2_03
Rhinecanthus_aculeatus_RH2x1
Mola_mola_KV751324_RH2_01
Mola_mola_KV751324_RH2_02
Tetraodon_nigroviridis_RH2
Takifugu_flavidus_CM011072_RH2_01
Takifugu_rubripes_NC_042303_LOC619285_RH2_02
Mastacembelus_armatus_NW_020535886_LOC113130119_RH2
Betta_splendens_NC_040885_LOC114855098_RH2_01
Betta_splendens_NC_040885_LOC114855097_RH2_02
Betta_splendens_NC_040885_LOC114855678_RH2_03
Monopterus_albus_NW_018127916_LOC109958953_RH2
Anabas_testudineus_NW_020535985_LOC113153882_RH2_01
Anabas_testudineus_NW_020535985_LOC113154539_RH2_02
Anabas_testudineus_NW_020535985_LOC113154538_RH2_03
Antennarius_maculatus_CM023609_RH2_01
Antennarius_maculatus_CM023609_RH2_02
Lophius_piscatorius_RH2x1
Lophius_piscatorius_RH2x2
Epinephelus_moara_CM016924_RH2_03
Epinephelus_aeneus_RH2_gen03
Sebastes_nigrocinctus_RH2_gen02
Sebastes_nigrocinctus_RH2_gen03
Sebastes_norvegicus_RH2_gen01
Sebastes_norvegicus_RH2_gen03_ex345
Carapus_acus_RH2_gen02
Sphaeramia_orbicularis_NC_043961_LOC115419197_RH2_03
Alticus_simplicirrius_B7_RH2x2
Sphaeramia_orbicularis_NC_043961_LOC115419196_RH2_04
Istiblennius_lineatus_B3_RH2x2_inkomp
Boleophthalmus_pectinirostris_RH2_C
Periophthalmus_magnuspinnatus_RH2_gen02
Lesueurigobius_sanzoi_RH2
Neogobius_melanostomus_con4222_RH2_01
Neogobius_melanostomus_con1118_RH2_02
Notolabrus_celidotus_CM019771_RH2_04
Cheilinus_undulatus_SRR11496420_LG03_RH2_1
Epibulus_insidiator_RH2A_KP881299
Symphodus_melops_RH2_gen0203gl
Labrus_bergylta_NW_018115345_LOC110002300_RH2_02
Labrus_bergylta_NW_018115345_LOC110002302_RH2_01
Cheilinus_undulatus_SRR11496420_LG03_RH2_2
Epibulus_insidiator_RH2A_KP881310
Labrus_bergylta_NW_018115345_LOC110002301_RH2_03
Symphodus_melops_RH2_gen01
Notolabrus_celidotus_CM019771_RH2_03
Notolabrus_celidotus_CM019771_RH2_05
Lateolabrax_maculatus_CP027280_RH2_01
Lateolabrax_maculatus_CP027280_RH2_02
Dicentrarchus_labrax_RH2_gen02_ex1234
Dicentrarchus_labrax_RH2_gen01_ex1345_pse
Dicentrarchus_labrax_RH2_gen03
Etheostoma_spectabile_NC_045736_LOC116687287_RH2_02
Etheostoma_spectabile_NC_045736_LOC116688203_RH2_01_pseudo_short_ex12
Etheostoma_spectabile_NW_022602544_LOC116674387_RH2_03
Cottoperca_gobio_NC_041359_LOC115007888_RH2_01
Cottoperca_gobio_NC_041359_LOC115007891_RH2_02
Notothenia_coriiceps_RH2
Chaenocephalus_aceratus_RH2_gen01
Chaenocephalus_aceratus_RH2_gen02
Trachinotus_ovatus_UWUD01000008_RH2_02
Trachinotus_ovatus_UWUD01000008_RH2_01
RH2A

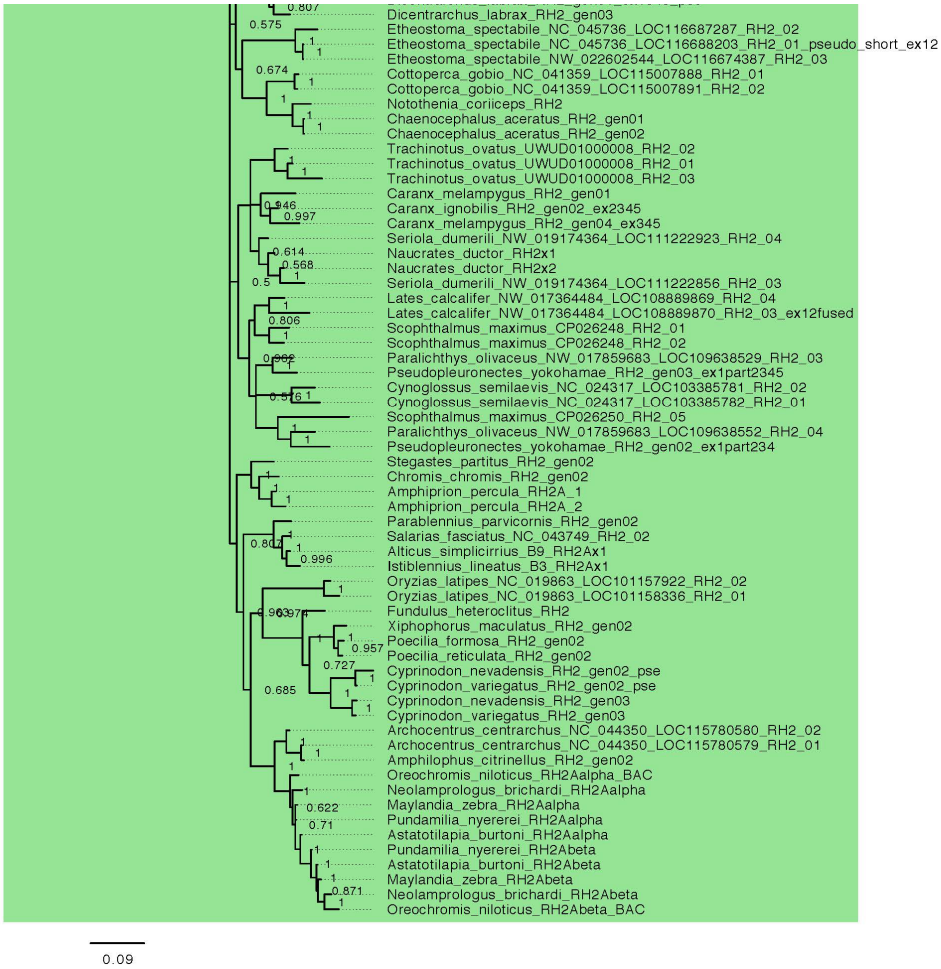

Supplementary Figure S1: *RH2* gene tree including all sequences mined from the whole genome dataset of 115 teleost species and three non-teleost outgroups.